Environmental Science and Pollution Research (2018) 25:20125–20140
https://doi.org/10.1007/s11356-018-2215-8

RESEARCH ARTICLE

Nanocomposite Au NP/TiO_2 thin film in the efficient remediation of aqueous solutions contaminated with emerging micro-pollutants

Lalliansanga Nil[1] · Alka Tiwari[2] · Alok Shukla[2] · Diwakar Tiwari[1] · Seung Mok Lee[3]

Received: 12 February 2018 / Accepted: 1 May 2018 / Published online: 10 May 2018

Abstract

The present communication specifically aims to synthesize novel nanocomposite material Au NPs/TiO_2 in a simple template process using the polyethylene glycol as filler media. The thin film of the nanocomposite material was characterized by the advanced analytical tools. The surface morphology was obtained by the scanning electron microscopic (SEM) and transmission electron microscopic (TEM) images of solids. Similarly, the surface topography and roughness of solid were obtained by the atomic force microscopic (AFM) image of thin film. X-ray diffraction (XRD) data enabled to confirm that the TiO_2 was predominantly present with its anatase phase. The specific surface area and pore size of the solid were obtained using the N_2 adsorption/desorption data. Nanocomposite Au NP/TiO_2 thin film was employed in the photocatalytic removal of sulfamethoxazole and triclosan from aqueous solutions using less harmful UV-A light (λ_{max} = 330 nm). Various physicochemical parametric studies enabled to deduce the mechanism involved in the degradation process. The degradation kinetics as a function of pH (pH 4.0–10.0) and micro-pollutant concentrations (0.5–15.0 mg/L) was extensively studied. The mineralization of these pollutants was obtained using the non-purgeable organic carbon (NPOC) data. The stability of thin film was assessed by the repeated operations, and presence of several co-existing ions simulates the studies to real matrix treatment. Further, the presence of scavengers enabled to pin point the radical-induced degradation of sulfamethoxazole and triclosan from aqueous solutions.

Keywords Emerging water pollutants · Nanocomposite Au NPs/TiO_2 · Degradation kinetics · Mineralization · Stability of catalysts

Introduction

The detection of several pharmaceuticals and personal care products (PCPs) in water bodies is found ubiquitous and widespread (Mompelat et al. 2009; da Silva et al. 2011; Wu et al. 2012). These water contaminants are persistent and found difficult to eliminate completely in the existing biological or physicochemical wastewater treatment plants. Hence, they are eventually escaped through the wastewater treatment plants (WWTPs), at low level, and subsequently enter into the fresh water system, contaminating the water bodies, viz., drinking water, surface water, or even the river/lake waters. Based on its toxicity or prevalence to drug resistance in the environment and human commensal microbes or due to persistence in nature, these compounds are known as emerging water pollutants (Constantin et al. 2018; Han et al. 2017). Although the regulatory bodies have not prescribed the permissible limit of these emerging pollutants in the water bodies, however, based on its potential risk towards the human being, animals or aquatic life, it is important to eliminate effectively from aqueous solutions (Kosera et al. 2017).

Sulfamethoxazole is one of widely used antibiotics which belongs to the sulfonamide group of antibiotics. This is included with the other antibiotics sulfadiazine, sulfamerazine, sulfamethazine sulfathiazole, and sulfapyridine (Kolpin et al. 2002a; Cheng et al. 2017). It was most detected (100%) water contaminants as monitored in 139 streams in the USA from

Responsible editor: Suresh Pillai

✉ Diwakar Tiwari
diw_tiwari@yahoo.com

[1] Department of Chemistry, School of Physical Sciences, Mizoram University, Aizawl 796004, India

[2] Department of Physics, National Institute of Technology, Aizawl 796001, India

[3] Department of Health and Environment, Catholic Kwandong University, 24, Beomil-ro 579beon-gil, Gangneung 210-701, South Korea

1999 to 2000 (Ahmed et al. 2015; Kang et al. 2018). Sulfamethoxazole possesses the log K_{ow} and pK_a values of 0.89 and 1.6/5.7, respectively. This antibiotic is widely used as bacteriostatic agent and frequently supplemented in human and veterinary medicines (Hu et al. 2007; Wang et al. 2018b). This is also prescribed as a synergistic additive with trimethoprim to treat urinary tract infections (Dias et al. 2014). The contamination of aquatic environment by the pharmaceuticals, in general, is mainly due to the wastewaters that originate from the hospitals, veterinary clinics, households, pharmaceutical manufacturing facilities, etc. Similarly, a large and significant contribution is from the wastes originating from the livestock as the feces and urine of animals contained with significant load of antibiotics (Behera et al. 2011). A report suggested that about 29.9 million pounds of antibiotics were used on farm animals (Leavey-Roback et al. 2016; Wang and Wang 2016). Since, only part of it is metabolized and *Ca* 70–90% is excreted through feces and urines as such or its metabolite forms (Massé et al. 2014). This subsequently enters as influent of WWTPs and eventually contaminates the water bodies.

On the other hand, the triclosan (5-Chloro-2-(2,4-dichlorophenoxy)phenol) is polychlorinated aromatic antimicrobial drug. It effectively inhibits the *enoyl-acyl* carrier protein reductase for fatty acid synthesis in bacteria, blocking lipid biosynthesis in *Escherichia coli* and promoting a mutation in a *FabI* gene (Heath et al. 2000; Heath and Rock 2000; Jones et al. 2000). It is often included as an additive for many health and personal care products (Sivaraman et al. 2003). Triclosan is introduced as a preservative or as an antiseptic agent for several consumer products of daily use, viz., hand soaps, skin creams, toothpastes, and household cleaners or even in textiles (Singer et al. 2002; Yang et al. 2011). It is reported that triclosan is less toxic, hence less health concerns; however, triclosan is readily photo-transformed in aqueous media and generating 2,8-dichloro-dibenzo 1,4-dioxincompounds which are potential carcinogens (Aranami and Readman 2007; Sanchez-Prado et al. 2006). Similarly, it was pointed that methyl triclosan occurred through the biological methylation was known to be more lipophilic and bioaccumulative than the parent triclosan compound (Lindström et al. 2002). The acidic dissociation constant (pK_a) of triclosan is ranged between 7.9 and 8.1; hence, the solubility of triclosan increases with the increase in pH (Grove et al. 2003). The octanol-water partition coefficient (log K_{ow}) was reported to be 5.4 that indicates the compound is a stable lipophilic (Hart 1999). Therefore, triclosan feebly accumulates in aquatic and terrestrial organisms (Son et al. 2009). Triclosan is one of abundantly detected contaminants in the aquatic environment (Huang et al. 2016; Thomaidi et al. 2017) and reported to be 57.6% in US streams and 62.7% in Elbe River water samples (Kolpin et al. 2002a). It is often detected in the human urine, plasma, breast milk, etc. samples (Adolfsson-Erici et al. 2002; Allmyr et al. 2006; Arbuckle et al. 2015). Triclosan is reported to be geno- and cytotoxic compound studied for the aquatic organisms and species such as algae and fish (Kolpin et al. 2002b). Another report indicated that triclosan itself shows weak androgenic activity towards aquatic life (Foran et al. 2000) and, hence, the estrogenic and androgenic responses in human breast cancer cells (Gee et al. 2008). These studies further demonstrated that triclosan is a potential endocrine-disrupting compound.

Therefore, the widespread and ubiquitous presence of these emerging water contaminants poses a serious environmental challenge to tune better the existing wastewater treatment technologies to eliminate these contaminants effectively. The role of advanced hybrid materials or metamaterials showed widespread applications in the area of electronics (Srinivasarao et al.; Guslienko 2008; Shankar et al. 2018; Sun et al. 2018), enhanced interfacial shear strength (IFSS) and tensile strength materials (Wang et al. 2017), mechanical properties (Liu et al. 2017), and electrically conducting thermoplastic materials (Liu et al. 2015, 2016, a; Hu et al. 2018; Li et al. 2018) or even in several environmental remediation strategies (Song et al. 2012; Ahmed et al. 2015). Similarly, the 2D photocatalysts were employed in the efficient water splitting process (Su et al. 2018). The composite materials based on titania were used for an enhanced catalytic activity or even in self-cleansing titania mesh membrane for efficient oil/water separation process (Zhang et al. 2017b; Kang et al. 2018). The antibacterial and bacterially adhesive cotton fabrics coated with cationic fluorinated polymer materials were synthesized by co-polymerization process (Lin et al. 2018). An interesting computer simulation study was overviewed to study the physical properties of several nanocomposite materials (Zhao et al. 2017). In a line, the advanced oxidation process integrated with the TiO_2 or titania-based photocatalysts is found to be an effective method to degrade the stable and potentially emerging micro-pollutants (Zhang et al. 2017a). The process includes with in situ generation of highly reactive hydroxyl radicals (rate constants in the order of 10^6 to 10^9 M^{-1} s^{-1}) that are predominantly responsible for the degradation/or even mineralization of micro-pollutants from wastewaters (Buxton et al. 1988; Zhang et al. 2017a, b). The variety of template materials were introduced in literature to synthesize several nanocomposites that include acrylonitrile-butadiene-styrene, polydimethylsiloxane, poly(acrylic acid), polyacrylonitrile, and poly(vinyl alcohol) (Li et al. 2017; Sun et al. 2017a; Ma et al. 2017; Wang et al. 2018a; X. Cui et al.). Literature survey further reveals that the graphene-based titanium oxide composite materials were found useful in the removal of antibiotics, viz., sulfamethoxazole (SMX), erythromycin (ERY), and clarithromycin (CLA), antibiotic-resistant bacteria, and their associated genes using the solar radiation. The results indicated that the composite materials could degrade ERY (84 ± 2%), CLA (86 ± 5%), and SMX (87

±4%) which were slightly higher than the pristine TiO_2 photocatalyst (Karaolia et al. 2018). Iron phthalocyanine is supported with activated carbon fiber (FeMATNPc) to enhance the catalytic degradation of sulfamethoxazole from aqueous solutions. The EPR results demonstrated that the radical species and the higher valent iron (Fe(IV)) were dominantly involved in the degradation of sulfamethoxazole (Wang et al. 2018b). Similarly, several photo-Fenton or Fenton-like processes were demonstrated in the removal of sulfamethoxazole using the materials Ce-Fe-graphene nanocomposite (Wan et al. 2016) or ferrioxalate complexes (Dias et al. 2014). On the other hand, a photoelectrocatalytic (PEC) process along with the UV illumination showed to achieve 78.7% removal of triclosan; however, the harmful intermediate 2,7-dichlorodibenzodioxin (DCDD) was formed in the degradation process (Liu et al. 2013). The TiO_2-based photocatalytic degradation of triclosan using the UV-A illumination showed a high percentage removal, and the kinetic studies showed that the degradation process followed the Langmuir–Hinshelwood model ($b = 27.99\ mM^{-1}$, $K_{triclosan} = 9.49\ mM^{-1}$) (Son et al. 2009). A CPC reactor (packed bed reactor type CPC) was packed with the TiO_2-impregnated tezontle stones, and it was then operated for the removal of triclosan using the solar radiations. This could achieve a removal efficiency of 74% in presence of persulfate as an effective electron acceptor (Martínez et al. 2014). TiO_2 (Degussa) photocatalyst was employed in the degradation of triclosan from aqueous solutions using the UV light ($\lambda < 365$), and it is interesting to observe that no dichlorophenol intermediate was formed in the photocatalytic degradation process (Yu et al. 2006). The heterogeneous zinc oxide (ZnO: crystal phase wurtzite) immobilized with sodium alginate showed fairly a high removal efficiency of triclosan within 20 min of contact whereas solar-irradiated sample required 90 min of contact to achieve the degradation efficiency 90% (Kosera et al. 2017). Similarly, the Fenton-like processes using the $BiFeO_3$ magnetic nanoparticles ($BiFeO_3$ MNPs) (Song et al. 2012) or ferric ion (Munoz et al. 2012) were introduced to achieve a high degradation efficiency of triclosan from aqueous solutions.

The TiO_2 catalyst decorated with the noble metal nanoparticles (NPs), viz., NPs of Ag or Au could absorb the photon in the visible region since these NPs enable to cause the surface plasmon resonance effect and stimulate the localized electric field in the vicinity of TiO_2 that results in facile generation of e^-/h^+ pairs at the surface of TiO_2 (Ihara et al. 1997). Additionally, the NPs on TiO_2 act as co-catalysts which promote the e^-/h^+ separations (Seery et al. 2007). The catalytic activity of TiO_2 largely depends upon the particle size, geometry, and the type of noble metal NPs doped in its sphere (El-Sayed 2001). Previously, the $BaTiO_3$ nanoparticles were synthesized by the thermohydrolysis route which provides a novel low-temperature route in the synthesis of perovskite films. The films possessed with a stable dielectric constant of 30 having the frequency ranged from 0 Hz to 1 MHz (Sun et al. 2017b). Similarly, the enhanced lithium ion batteries were obtained using the nanocomposites of $TiNb_2O_7$/carbon nanotubes or nanoparticles of $FeNb_{11}O_{29}$ as anode materials (Lou et al. 2017; Hou Qinzhi et al. 2018). In a line, the TiO_2 thin films are a viable option of utilizing the photocatalysts in the treatment of wastewater treatment plants that makes the phase separation easy and possesses greater applicability in the repeated catalytic operations. However, the impregnation of NPs with TiO_2 network in thin film is a challenging objective. A simple deposition of NPs is found unstable under reaction conditions, and it readily migrates and aggregates to the larger particles. This causes the loss of its unique properties (Huang et al. 2017). Therefore, present communication aims to synthesize a Au NP/TiO_2 nanocomposite thin film with the template synthetic method. Further, the nanocomposite material was employed in the remediation of aqueous solutions contaminated with emerging water pollutants, viz., sulfamethoxazole and triclosan. The detailed physicochemical parametric studies enabled to deduce the mechanism of degradation, and kinetic studies revealed the efficiency of nanocomposite materials in the degradation process.

Materials and methods

Chemical and materials

Gold(III) chloride hydrate, triclosan (99.999%), sulfamethoxazole, acetic acid (99%), and sodium borohydride (98%) were obtained from the Sigma-Aldrich. Co., USA. Titanium (IV) isopropoxide (99%) and polyethylene glycol (average molecular weight 800) were obtained from the Samchun Pure Chemical Co. Ltd., Korea. Sodium nitrate and ethylenediaminetetraacetic acid disodium salt was obtained from Loba Chemicals, India. Ethanol anhydrous was obtained from the Daejung Chemicals & Metals Co. Ltd., Korea. Sodium chloride, sodium azide, oxalic acid dihydrate, sodium hydrogen carbonate, 2-propanol, zinc chloride dry, cadmium nitrate tetrahydrate, copper (II) sulfate pentahydrate, glycine, and acetonitrile (HPLC grade) were obtained from the Merck India Ltd., India. Purified water (18.2 MΩ cm at 25 °C) was collected from the Millipore Water Purification system (model: Elix 3).

UV-visible spectrophotometer (Thermo Fisher Evolution Model-220, UK) was employed for the spectrophotometric determination of sulfamethoxazole or triclosan in aqueous solutions. The sulfamethoxazole and triclosan give the distinct absorption peaks at the wavelength (λ_{max}) 360 and 254 nm, respectively. The standard solutions of sulfamethoxazole or triclosan were prepared having the micro-pollutant concentrations 0.5, 1.0, 5.0, 10.0, and 15.0 mg/L. Calibration lines were drawn between the concentrations of these standard solutions

and its corresponding measured absorbance (correlation coefficient $R^2 = 0.999$). The total organic carbon (TOC) analyzer (Shimadzu, Japan; model: TOC-VCPH/CPN) was employed to measure the non-purgeable organic carbon (NPOC) values to study the, possible, mineralization of sulfamethoxazole or triclosan from aqueous solutions by the photolytic/or photocatalytic treatments. A UV-A lamp, wavelength (λ_{max}) = 360 nm (model: 9W, PLS9W BLB/2P 1CT, Philips), was obtained from the Hansung UV Pvt. Co. Ltd., Korea.

Methodology

Synthesis of gold nanoparticles

Nanoparticles of gold were obtained by using previously described method (McFarland et al. 2004). Briefly, 0.1 mmol/L of gold(III) chloride solution was prepared in distilled water. Fifty-milliliter gold(III) solution was taken into a conical flask and was heated up to its boiling. Then slowly, under the stirred conditions, 2-mL 1% trisodium citrate solution was added quickly to the gold(III) solution. The solution was taken off from the hot plate. The gold(III) rapidly reduces to Au(0) and the color of the solution was quickly changed to deep red. The gold nanoparticles were formed and it was found stable for hours.

Synthesis of Au/titania sol

A template synthesis of TiO_2 was carried out using the titanium alkoxide precursor. The polyethylene glycol was introduced as a template to generate titania network. Titanium(IV) isopropoxide 28 g was mixed with 13 g of acetylacetone and 2 g of polyethylene glycol was dissolved in it. Simultaneously, freshly prepared 10 mL of Au(0) nanoparticle suspension was mixed. Further, a solution mixture of ethanol (184 g), acetic acid (5.8 g), and distilled water (22.5 g) was mixed slowly to the titanium solution. The solution mixture was stirred vigorously for 2 h followed by sonication for 30 min in a sonication bath. A clear sol Au NP/TiO_2 was obtained which was aged for Ca. 24 h and employed for the fabrication of thin films.

Preparation of nanocomposite Au NP/TiO_2 thin film

Borosilicate glass disk (2.3 cm diameter and 0.5 mm thickness) was cleaned by 0.1 mol/L HNO_3 and washed repeatedly by the distilled water and dried in a drying oven. Further, the disk was taken slowly in the transparent solution of Au NPs/TiO_2 and placed vertically in the titania sol for 1 h. It was then taken out slowly using a forceps. The disk was kept in air for *Ca* 12 h and then dried first at 100 °C for 1 h followed by annealing at 500 °C for 3 h in an electric furnace (Nabertherm; model no. LT/15/12/P330, Germany). This results a very fine thin film formation of nanocomposite Au NPs/TiO_2 onto the substrate surface. Further, the process was repeated for another two times that enables to obtain a fine and smooth thin film formation onto the surface. The thin film samples were stored in a vacuum desiccator under dark conditions for its further use as photocatalyst.

Further, the solvents of sol solution Au NPs/TiO_2 were evaporated at 105 °C followed by annealing at 500 °C to obtain the nanocomposite Au NP/TiO_2 solid. The solid was crushed in a mortar to obtain the fine powder of material. It was kept in the airtight polyethylene bottle.

Morphological study of material

The surface morphology of thin film Au NPs/TiO_2 was obtained by the scanning electron microscope (SEM) machine (model FE-SEM SU-70, Hitachi, Japan). Similarly, the nanocomposite Au NP/TiO_2 powder was subjected for the transmission electron microscopic (TEM) analysis using the TEM analyzer (Tecnai F20 Transmission Electron Microscope, FEI, USA). The topographical 3D image of thin film was obtained by the atomic force microscope (AFM) machine (XE-100 apparatus from Park Systems, Korea) having sharp tips (>8 nm tip radius; PPP-NCHR type from Nanosensors™). The images were taken over the area of $10 \times 10\ \mu m^2$ and it was conducted in a non-contact mode. The 3D data clearly enabled the pillar height of TiO_2 along with the surface roughness.

Characterization of thin films

The X-ray diffraction (XRD) data of Au NP/TiO_2 thin film was collected using the X-ray diffraction machine (i.e., PANalytical, Netherland; model X'Pert PRO MPD). It was recorded at the scan rate of 0.033 of 2θ illumination and having the generator settings 30 mA, 40 kV. The $CuK_{\alpha 1}$ and $CuK_{\alpha 1}$ radiations were employed having wavelengths of 1.5406 and 1.54443 Å. The BET specific surface area was obtained using BET surface area analyzer (model ASAP 2020; Protech Korea) based on the liquid N_2 adsorption and desorption method.

Photocatalytic removal of micro-pollutants

Stock solutions of sulfamethoxazole or triclosan (each 20.0 mg/L) were prepared in a purified water. In order to increase the solubility of these micro-pollutants, the solutions were sonicated for 10 min in a sonication bath. Further, the required experimental concentrations of sulfamethoxazole or triclosan were obtained by the successive dilution of each stock solution. The pH of micro-pollutant solution was adjusted by the dropwise addition of conc. HCl/NaOH solutions. The concentration dependence data was collected by varying each micro-pollutant concentrations from 1.0 to 15.0 mg/L.

In order to conduct the photolytic or photocatalytic operations, a self-assembled photo reactor was used. A black box (dimension 60 × 45 × 45 cm) was made by cardboard and wrapped with black paper. A borosilicate glass beaker (100 mL) was contained with 50.0 mL of micro-pollutant solution and was placed inside the black box. Carefully, the nanocomposite Au NP/TiO_2 thin film disk was placed horizontally at the bottom of the reactor vessel. A UV-A lamp was mounted *Ca* 10 cm above to the micro-pollutant solution. The UV-A radiations enter the photocatalyst through the pollutant solution that enables the photocatalytic oxidation of micro-pollutants, i.e., sulfamethoxazole or triclosan. The temperature of reactor was maintained to 25 ± 1 °C using a self-assembled water bath. The sample solution was taken out from the reactor at definite time intervals in order to analyze the micro-pollutant concentrations using a UV-Vis spectrophotometer. Always a blank experiment was performed using only UV-A irradiation without the thin film photocatalyst for comparison of photocatalytic degradation of these micro-pollutants.

Results and discussion

Morphological study of thin films

The SEM image of Au NP/TiO_2 thin film is shown in Fig. 1a. Figure 1a clearly indicated that fine grains of TiO_2 are distributed on the surface of borosilicate glass-making thin film of composite material of Au NPs/TiO_2. Very heterogeneous surface structure is visible on the surface having some cracks at places. Moreover, some of the mesopores are also seen on the surface. Interesting to note that at places, the Au(0) nanoparticles are visible with the TiO_2 structure. A similar Au(NPs) were impregnated/decorated with the TiO_2 nanotubes using the two-step anodization method. The Au nanoparticles were clustered at the TiO_2 surface, and the density of gold clusters depends largely on the gold concentrations along with the bias voltages (Noothongkaew et al. 2017).

The TEM image of the powder nanocomposite Au NPs/TiO_2 was taken and presented in Fig. 1b. It is evident from the TEM image that the Au nanoparticles are distributed with the TiO_2 network. The particle size was ranged within 25–30 nm. Further, the interplanar distance of the Au Nanoparticles was estimated to be 0.25 nm for the solid sample of Au NPs/TiO_2. It was reported previously that Au (NPs) are well dispersed with the spherical surface of SiO_2 having a mean diameter of about 3–5 nm, and the interplanar distance of Au NP adjacent lattice planes was measured to be 0.32 (Huang et al. 2017). The other studies also indicated that the average Au particles were ranged between 3 and 5 nm on the TiO_2 catalyst surface (Nguyen et al. 2008).

Further, the TEM/EDX elemental mapping was conducted for the nanocomposite material Au NPs/TiO_2 and results are illustrated in Fig. 1c. The EDX mapping was recorded for the elements titanium (Ti), oxygen (O), and gold (Au). The figure clearly demonstrated that the oxygen is intimately associated with Ti that confirmed the presence of TiO_2 and forming a chemical bond between the titanium and oxygen (Ti-O). Moreover, it is evident from the figure that the Au

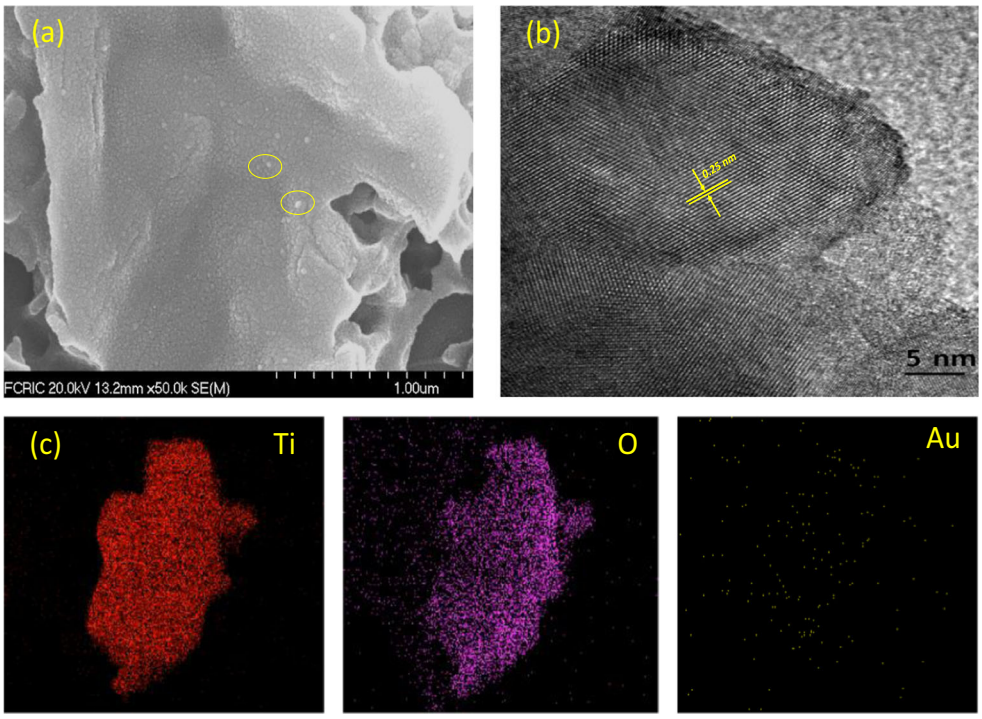

Fig. 1 **a** SEM image, **b** TEM image, and **c** TEM elemental mapping of the nanocomposite Au NPs/TiO_2

nanoparticles are very evenly and distinctly distributed within the titanium dioxide network. The Au^0 nanoparticles are not aggregated on the surface of titanium dioxide. Therefore, the in situ impregnation of Au nanoparticles enabled to distribute evenly within the titanium dioxide network. Similar EDX results were reported for the composite material TiO_2-Pt/graphene oxide solid that confirms the presence of Ti, O, Pt elements, and uniform distribution of Pt nanoparticles over the graphene sheets. The results further inferred that the intimate contact within these components has provided an enhanced photocatalytic activity of catalyst by the efficient carrier mobility (Rosu et al. 2017).

Further, a 3D atomic force microscopic image of nanocomposite Au NP /TiO_2 thin film is obtained and shown in Fig. 2. It is observed that TiO_2 is forming a very disordered heterogeneous structure on the surface. Moreover, it is pillared on the surface and the average pillar height was found to be *Ca* 600 nm. Further, the root mean square roughness (Rq) and mean roughness (Ra) were found to be 124.330 and 94.659 nm, respectively. It is evident again that the template synthesis enabled to synthesize a good heterogeneous surface structure with an enhanced pillar height of TiO_2.

Characterization of thin films

The X-ray diffraction data was collected for the nanocomposite Au NP/TiO_2 thin film. Results are shown in Fig. 3. The figure clearly reveals that the material is having predominantly amorphous in nature. This is because the material was not annealed at required high temperature. However, characteristic peak was observed around the 2θ value of 25.5 indicated the presence of anatase phase of TiO_2 (Shorke et al. 2018).

Further, the BET specific surface area, pore volume, and pore sizes of nanocomposite Au NPs/TiO_2 were obtained by the usual N_2 adsorption/desorption method. The N_2 adsorption/desorption curves are illustrated in Fig. 4. Adsorption/desorption isotherms revealed that it possessed the hysteresis loop of H2 type, which indicated the pores are having narrow mouths and cannel-like (Mendioroz et al. 1987; Seaton 1991). The pore size, pore volume, and the specific surface area of nanocomposite Au NPs/TiO_2 were found to be 5.60 nm, 0.034 cm^3/g, and 19.91 cm^2/g, respectively. Therefore, the material was possessed with good mesoporosity.

Photolytic and photocatalytic removal of triclosan and sulfamethoxazole

pH dependence study

The pH dependence degradation of sulfamethoxazole and triclosan was conducted as a function pH and illustrated in Fig. 5. Simultaneously, the speciation of sulfamethoxazole and triclosan was carried out and presented in Fig. 5. The pH dependence degradation of micro-pollutants greatly influenced with the species distribution of these micro-pollutants as well as the surface properties of solid catalyst. The photocatalytic processes largely depend upon the sorption of these species onto the catalyst surface. Figure 5 clearly demonstrated that the increase in pH caused for decrease in percentage removal of both the micro-pollutants from aqueous solutions. More quantitatively, increasing the pH from 4.0 to 10.0, the pollutant degradation was decreased from 64.45 to 55.18% (for sulfamethoxazole) and from 60.94 to 40.63% (for triclosan), respectively.

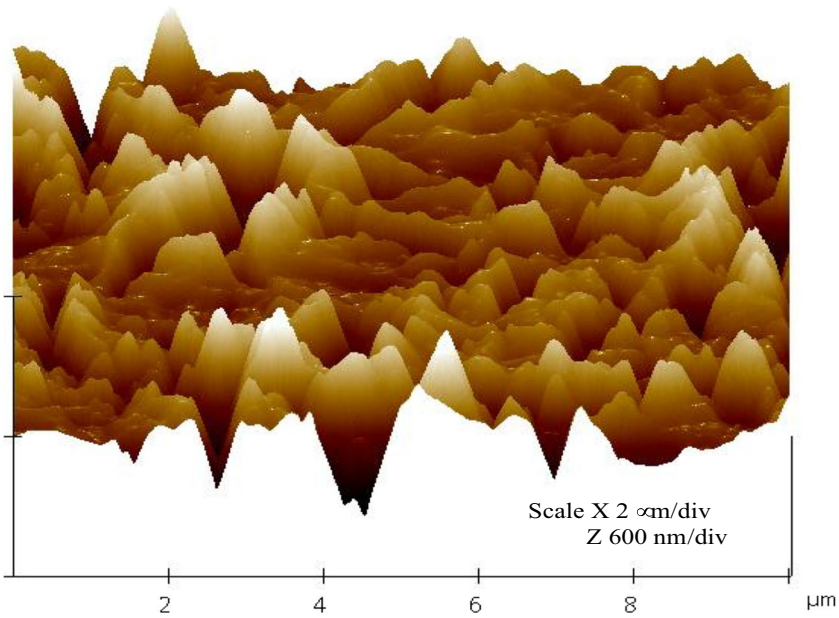

Fig. 2 Atomic force microscopic image of nanocomposite Au NP/TiO_2 thin film

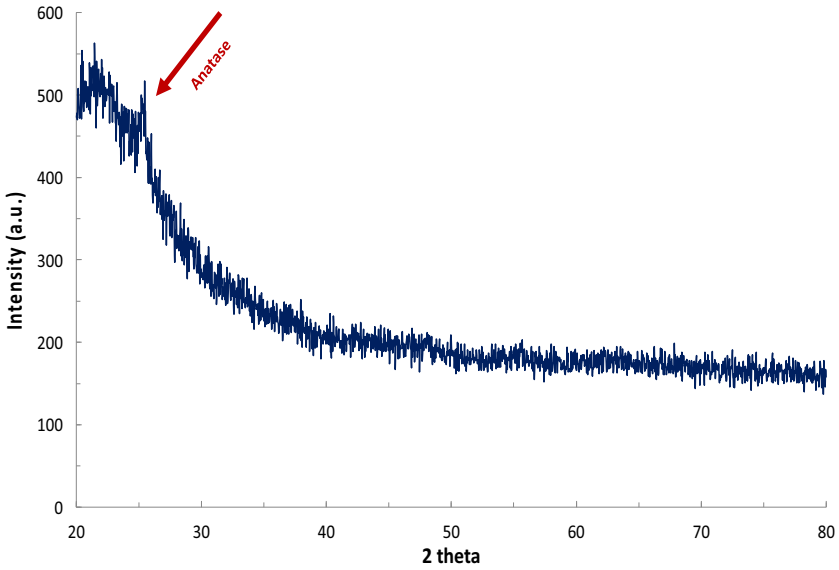

Fig. 3 X-ray diffraction pattern of nanocomposite Au NP/TiO_2 thin film

It was reported that the sulfamethoxazole (SMX) is having two dissociable hydrogens with the acid dissociation constant values pK_a^1 and pK_a^2, respectively 1.8 and 5.6 (Lucida et al. 2000). Therefore, the speciation studies revealed that above pH 3.6, the sulfamethoxazole is dominantly present with anionic species either SMX(-) or SMX(2-) (cf Fig. 5). Below pH 3.8, it partly exists as neutral sulfamethoxazole species of SMX(0). On the other hand, the pH_{PZC} (point of zero charge) values of anatase TiO_2 lie within the pH 4.8 to 6.5 with an accepted average value of 5.9. This indicated that the TiO_2 surface carries a net positive charge below pH 5.9, and eventually with the dissociation of proton, it turns to dissociated species and carries net negative charge above pH 5.9 as depicted in Eq. (1):

$$\equiv Ti{-}OH_2^{+} \leftrightarrow \underset{pH_{PZC}}{\equiv T{-}} OH^0 \leftrightarrow \equiv Ti{-}O^{-} \quad (1)$$

This indicates that at moderate to high pH values, i.e., pH > 5.9, both the surface and sulfamethoxazole species are negatively charged; hence, it electrostatically repels to each other. This causes less sorption of sulfamethoxazole onto the catalyst surface; therefore, a reduced degradation of sulfamethoxazole at high pH value is recorded. However, an increased degradation of sulfamethoxazole at low pH value, i.e., at pH 4.0, is due to the fact that the negatively charged sulfamethoxazole species are strongly sorbed onto the positively charged TiO_2 surface which favored the degradation of sulfamethoxazole.

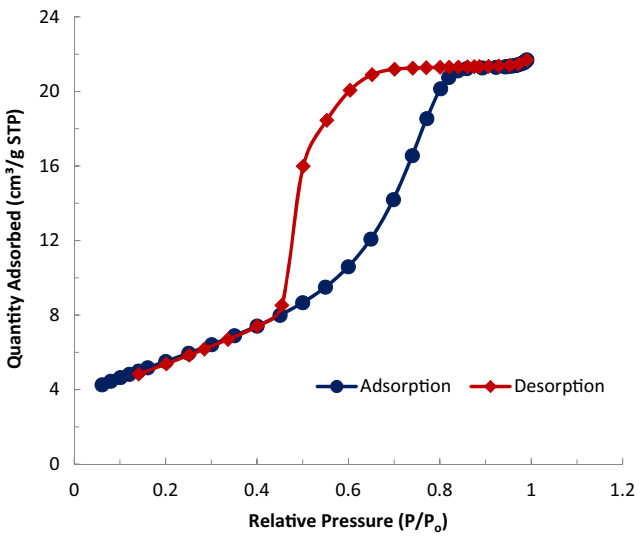

Fig. 4 BET adsorption/desorption isotherms of the nanocomposite Au NP/TiO_2 powder

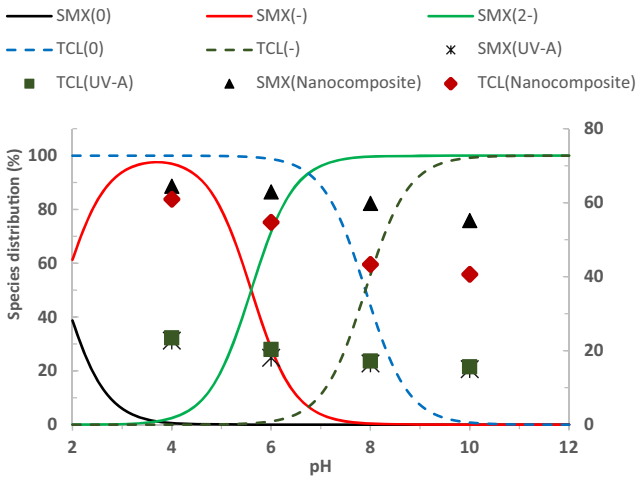

Fig. 5 Percentage distribution of species of sulfamethoxazole (smooth line) and triclosan (dotted lines) as a function of pH (Primary axis) and percentage removal of sulfamethoxazole and triclosan as a function of pH (Secondary axis) under the photolytic and photocatalytic operations [initial concentration of micro-pollutants, 1.0 mg/L]

Similarly, pH dependence sorption of sulfamethoxazole by the carbon nanotubes (CNT) was demonstrated under the fixed bed column reactor studies (Tian et al. 2013). It was pointed previously that the •OH radicals are having the same degradation tendency towards the anionic or neutral species of sulfamethoxazole; hence, a constant rate was obtained, i.e., $k_{SH,\bullet OH}$ and $k_{S^-,\bullet OH}$ having the value of $(7.63 \pm 0.85) \times 10^9$ M^{-1} s^{-1} (Yang et al. 2017). Other studies revealed that in a Fenton-like process, a similar less degradation of sulfamethoxazole was obtained at higher pH values employing the zero-valent iron under the oxic and anoxic environment (Kobayashi et al. 2017).

On the other hand, triclosan is a monoprotic acid and having the acid dissociation constant pK_a value 7.9 (Muzvidziwa et al. 2017). Hence, triclosan predominantly exists as a neutral species below pH 7.9 and pH > 7.9; it turns to the anionic species (cf Fig. 5). Therefore, increasing the pH causes a decrease in the sorption of triclosan by the TiO_2 surface; hence, a decreased degradation percentage of triclosan is obtained at high pH values, i.e., pH 8~10. These results further indicated that the neutral species of triclosan is readily degraded by the photocatalytic degradation. This is possibly due to the affinity of neutral triclosan species towards the TiO_2 surface, and the neutral species are less stable compared to the anionic species of triclosan. The results are in a line to the other reports indicated that a decrease in pH from 7.0 to 10.0 greatly decreased the pseudo-second-order rate constant (k_{app}) values in the degradation of triclosan by ferrate(VI) (Yuval et al. 2017). Moreover, the sorption of triclosan by the carbon nanotube (CNT) and functionalized CNT was decreased with the increase in pH (Li et al. 2017).

Further, it was noted that significantly less degradation of sulfamethoxazole or triclosan was obtained with the photolytic process at all studied pH compared to the photocatalytic process conducted with using the nanocomposite Au NP/TiO_2 thin film (cf Fig. 5). This clearly demonstrated that the thin film nanocomposite Au NPs/TiO_2 showed a greater catalytic activity that enabled to enhance the degradation percentage of sulfamethoxazole or triclosan from aqueous solutions. Moreover, increasing the pH from 4.0 to 10.0, a marked decrease in percentage degradation of these micro-pollutants is recorded. More quantitatively, increasing the pH from 4.0 to 10.0, the percentage degradation of sulfamethoxazole is decreased from 22.72 to 14.99, respectively. Similarly, the triclosan removal was decreased from 23.44 to 15.63% for the similar increase in pH. These results are pointed that the anionic species of sulfamethoxazole or triclosan are more stable than the neutral species of these micro-pollutants.

Concentration dependence removal of micro-pollutants

The initial concentration of sulfamethoxazole and triclosan was increased from 0.5 to 15.0 mg/L at constant pH 6.0. The micro-pollutants were treated for a constant time interval of 2 h using UV-A lamp. The percentage removal of sulfamethoxazole or triclosan was recorded and presented as a function of micro-pollutant concentration in Fig. 6. It is evident from the figure (Fig. 6) that increasing the micro-pollutant concentration significantly decreases the percentage removal of both the micro-pollutants, viz., sulfamethoxazole or triclosan, from aqueous solutions for the photolytic or photocatalytic processes. Increasing the concentration of micro-pollutant from 0.5 to 15.0 mg/L has caused to decrease the percentage removal of micro-pollutant from 75.27 to 35.60% (for sulfamethoxazole) and from 71.87 to 22.19% (for triclosan), respectively, using the nanocomposite Au NP/TiO_2 thin film. This decrease in percentage removal of micro-pollutants with the increase in initial concentration of micro-pollutant is explained with the fact that the contact possibilities of pollutants to the catalyst surface are relatively high at lower pollutant concentrations. Additionally, the catalyst surface contained with relatively higher percentage of surface active sites for lower number of total pollutant species present at lower concentration of pollutant (Lalhriatpuia et al. 2015). Moreover, the high concentration of pollutant species scavenges the catalyst activity; hence, a lower removal of pollutant was obtained at higher concentration of pollutants (Nasseri et al. 2017). Similarly, the results indicated that the photolytic degradation of sulfamethoxazole or triclosan is significantly less than the corresponding photocatalytic removal of these pollutants using the nanocomposite Au NP/TiO_2 thin film. This further inferred the potential catalytic activity of nanocomposite in the degradation of these emerging water contaminants.

Kinetic studies of micro-pollutant degradation

The time dependence photolysis or photocatalytic degradation of sulfamethoxazole and triclosan was carried out, and the observed values were modeled with a known pseudo-first-

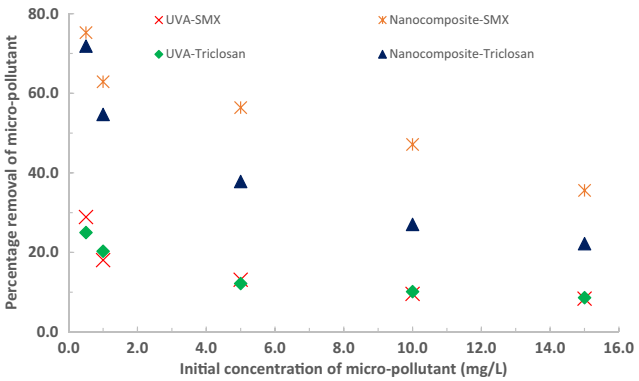

Fig. 6 Percentage removal of sulfamethoxazole and triclosan at various initial concentrations of micro-pollutants under the photolytic and photocatalytic processes using the nanocomposite Au NP/TiO_2 thin film photocatalyst [pH 6.0]

order rate equation (Tiwari et al. 2015). The kinetics was performed at all studied concentrations and at pH 6.0.

The pseudo-first-order rate constant (k_{app}) values were obtained at all the studied concentrations and presented in Fig. 7. The linear and non-linear (exponential) fitting for the pseudo-first-order rate equations was conducted to obtain the pseudo-first rate constant values for both the micro-pollutants, viz., sulfamethoxazole and triclosan, and the fitting data is shown in insets of Fig. 7. It is evident from Fig. 7 that a decrease in micro-pollutant concentration from 15.0 to 0.5 mg/L was apparently favored the rate constant values. More quantitatively, decreasing the concentration of sulfamethoxazole from 15.0 to 0.5 mg/L had caused to increase the pseudo-first-order rate constant values from 2.9×10^{-3} to 9.7×10^{-3} min^{-1}, respectively, using the nanocomposite Au NP/TiO_2 thin film. Similarly, for a similar decrease in triclosan concentration, the rate constant value was decreased from 1.7×10^{-3} to 8.8×10^{-3} min^{-1}, respectively, using the photocatalyst thin film. On the other hand, the pseudo-first-order rate constant values obtained for the photolytic degradation of sulfamethoxazole or triclosan are significantly lower than the corresponding rate constant values obtained for the photocatalytic degradation of these micro-pollutants (cf Fig. 7). This again reaffirmed the utility of nanocomposite Au NP/TiO_2 thin film photocatalyst in the removal of sulfamethoxazole or triclosan in aqueous solutions. A similar pseudo-first-order kinetics was obtained for the photocatalytic degradation of dyes (methylene blue, rhodamine B, eosin Y, and Congo red) from aqueous solutions using the CuS (NPs) photocatalyst (Ayodhya et al. 2016). Similarly, the triclosan degradation by the electro-Fenton process showed to be the pseudo-first-order rate kinetics (Sirés et al. 2007).

Further, it is interesting to find that the photocatalytic degradation of sulfamethoxazole and triclosan followed the known Langmuir–Hinshelwood (L-H) isotherm to its linear form at the studied concentrations (Lalhriatpuia et al. 2015). The L-H adsorption constant "K" (L/mg) and the rate constant "k_r" (mg/L/min) values were estimated and found to be 0.167 and 6.02×10^{-2} (R^2 0.979; for sulfamethoxazole) and 0.384 and 2.64×10^{-2} (R^2 0.984; for triclosan), respectively, using the nanocomposite Ag NPs/TiO_2 thin film. These results inferred that the photocatalytic degradation of these micro-pollutants fairly well demonstrated with the L-H kinetic modeling.

NPOC removal of micro-pollutants

The removal of micro-pollutants was intended to its mineralization, and the percentage mineralization of sulfamethoxazole or triclosan was obtained for the photolysis or photocatalytic processes. Therefore, the non-purgeable organic carbon (NPOC) data was collected for the treated aqueous samples. Using the initial NPOC values of micro-pollutants, the percentage mineralization was obtained at different pH values. The initial concentration of these micro-pollutants was kept constant 1.0 mg/L and the total illumination time was 2 h. The results were presented in Fig. 8. Figure 8 clearly demonstrated that increasing the solution pH, i.e., pH 4.0–10.0, had caused to decrease significantly the percent mineralization of these two pollutants. Quantitatively, increasing the pH from 4.0 to 10.0 the respective decrease in percentage NPOC removal was decreased from 54.30 to 39.49% (for sulfamethoxazole) and from 32.29 to 26.84% (for triclosan), respectively, using the nanocomposite Au NP/TiO_2 thin film photocatalyst. On the other hand, the photolytic mineralization of these two pollutants was obtained significantly less than the corresponding photocatalytic degradation. Although, a partial but significant amount of the micro-pollutants was mineralized in the photocatalytic process, however, a complete mineralization could be achieved with a prolonged or multiple operations of the process. The NPOC removal results were quite in a line to the results obtained for the degradation of pollutants in the concentration dependence studies.

Repeated use of thin film catalyst

The nanocomposite Au NP/TiO_2 thin film was subjected for the repeated photocatalytic operations, i.e., at least six-cycle operations, and results are presented in Fig. 9. The thin film was washed with distilled water and dried in a drying oven at 105 °C for 3 h and again was used for the next cycle of operation. The initial concentration of micro-pollutant was taken 5.0 mg/L with a constant pH 6.0. The results clearly demonstrated (Fig. 9) that even at the end of six cycle of operations, the percentage efficiency of photocatalyst was not hampered and almost an identical removal of sulfamethoxazole or triclosan was obtained. More quantitatively, at the completion of six cycles, the percentage removal of sulfamethoxazole was decreased from 55.24 to 54.60% (i.e., a decrease of 0.64%). Similarly, the triclosan percentage removal was decreased from 36.22 to 35.26% only (i.e., a decrease of 0.96%) at the end of six cycles of operations. These results showed that fairly a good stability of nanocomposite Au NP/TiO_2 thin film was achieved at least in successive operations of photocatalytic treatment. This eventually enhanced the applicability of the nanocomposite thin film in the wastewater treatment. It was reported previously that methyl orange removal using the TiO_2 supported on spherical activated carbon (TiO_2/SAC) was significantly decreased even at the completion of five cycles of operations (Yoon et al. 2012).

Presence of co-existing ions

Further, the presence of several co-exiting ions in the removal of micro-pollutants is an important parameter which simulates the study to the real matrix treatment. Therefore, the study was

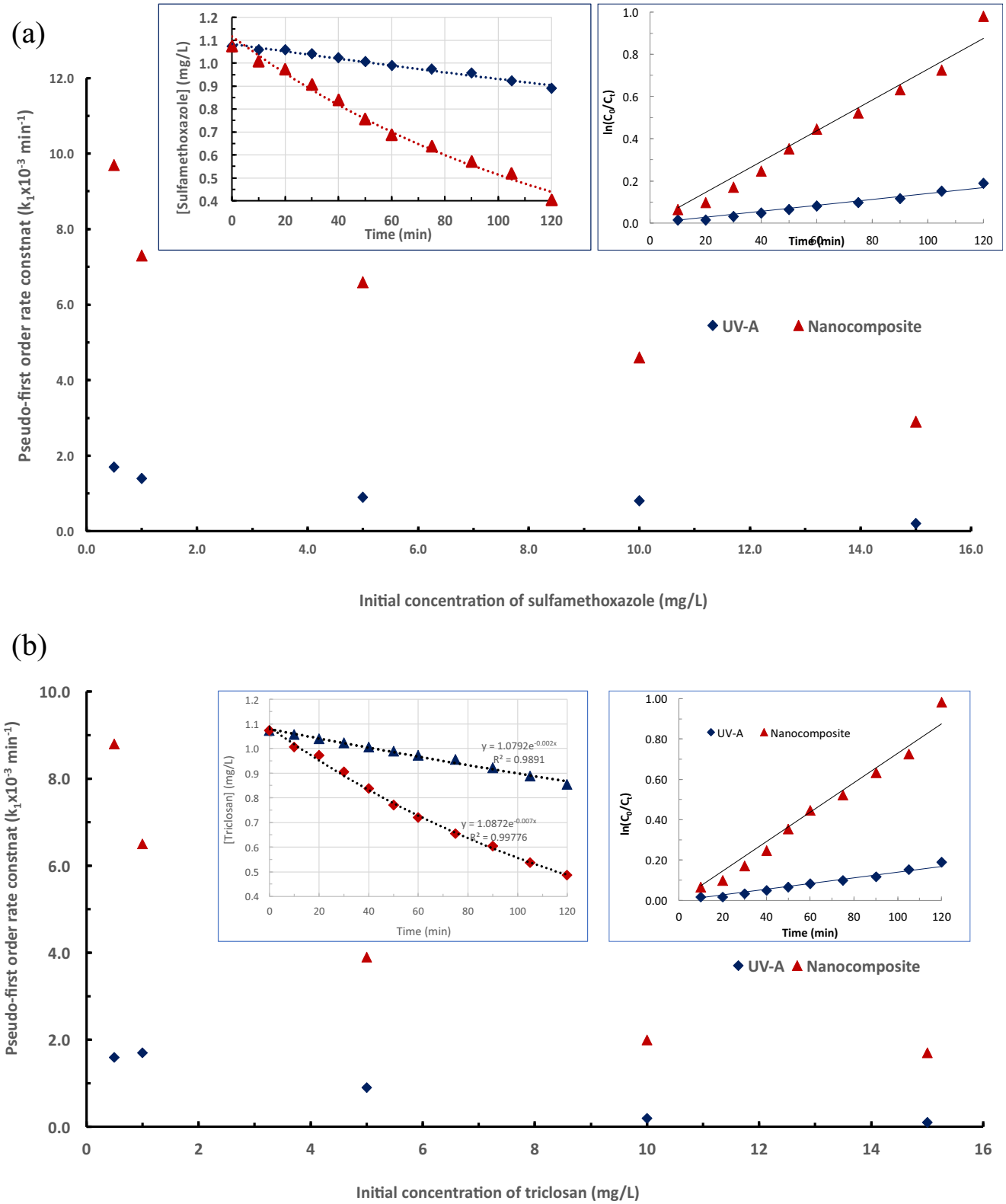

Fig. 7 The pseudo-first-order rate constant at varied concentrations of **a** sulfamethoxazole and **b** triclosan under the photolytic and photocatalytic processes [insets, linear and non-linear fitting of data for the pseudo-first-order rate kinetics; initial concentration of micro-pollutants 1.0 mg/L and pH 6.0]

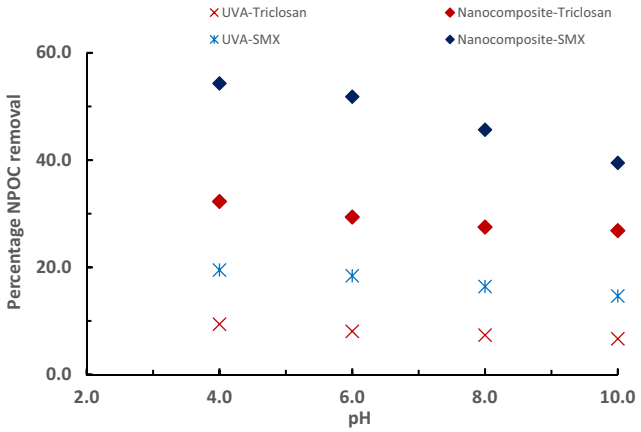

Fig. 8 Percentage removal of total NPOC of sulfamethoxazole and triclosan as a function of pH under the photolytic and photocatalytic degradation processes [initial concentration of micro-pollutant 1.0 mg/L]

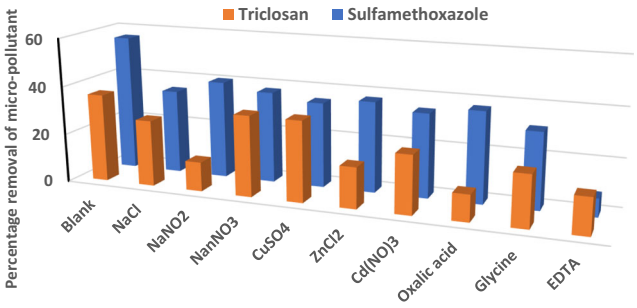

Fig. 10 Photocatalytic removal of sulfamethoxazole and triclosan in presence of several co-existing ions using the nanocomposite Au NP/TiO_2 thin film photocatalyst ([micro-pollutant] 5.0 mg/L; [co-ions] 50.0 mg/L; pH 6.0)

extended to assess the photocatalytic degradation of sulfamethoxazole and triclosan from aqueous solutions in presence of several co-existing cations and anions, viz., NaCl, $NaNO_3$, $NaNO_2$, $CuSO_4$, $Cd(NO_3)_2$, $ZnCl_2$, glycine, oxalic acid, and EDTA using the Au NP/TiO_2 photocatalyst. The initial concentration of sulfamethoxazole and triclosan was taken 5.0 mg/L and pH 6.0. The total illumination time was provided 2 h. Moreover, the co-existing ion concentration was taken 50.0 mg/L. The percentage of degradation of these micro-pollutants in presence of co-existing ions is presented in Fig. 10. The figure clearly revealed that the presence of these ions affected to a greater or lesser extent the degradation of sulfamethoxazole or triclosan. However, it is interesting to note that the presence of EDTA, $NaNO_2$, and oxalic acid had caused to suppress significantly the degradation of triclosan. Similarly, the presence of EDTA affected the degradation of sulfamethoxazole in the photocatalytic degradation process. The presence of other ions was affected to a lesser extent in the photocatalytic degradation of these two micro-pollutants.

Radical scavenger study

The 2-propanol and HCO_3^- molecules readily scavenge the •OH radicals in aqueous solutions (Xu et al. 2015; Lalhriatpuia et al. 2015). Similarly, the EDTA could scavenge the h^+ in TiO_2 semiconductor (Jia et al. 2017), and sodium azide (NaN_3) suppresses the singlet oxygen that occurred by the interaction of superoxide radical and photogenerated holes. The singlet oxygen readily degrades the organic compounds in aqueous media (Barka et al. 2010). Therefore, the photocatalytic degradation of sulfamethoxazole and triclosan (initial concentration of each pollutant 5.0 mg/L and pH 6.0) in presence of 2-propanol, HCO_3^-, and sodium azide (each one is having 1000 mg/L) was carried out using the nanocomposite Au NP/TiO_2 thin film photocatalyst. The percentage removal of sulfamethoxazole or triclosan in presence of these

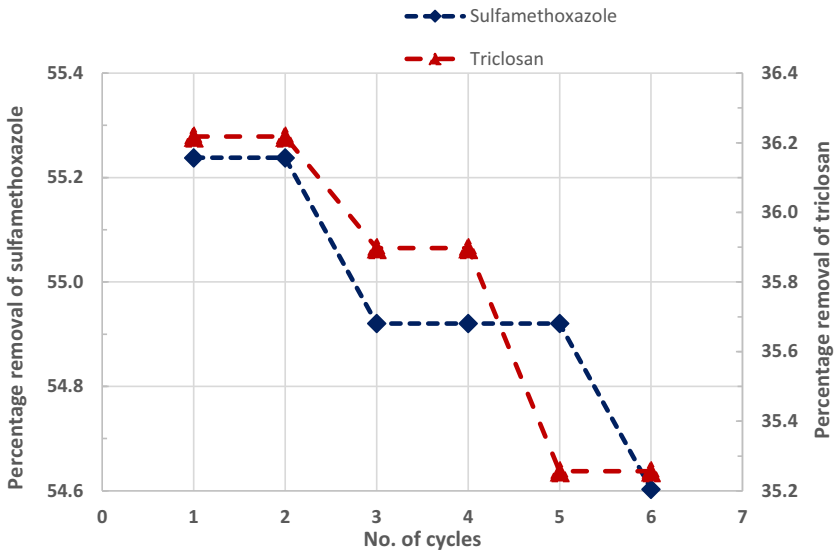

Fig. 9 Repeated use of nanocomposite Au NP/TiO_2 photocatalyst in the photocatalytic removal of sulfamethoxazole and triclosan using the UV-A illumination [initial concentration of micro-pollutant 5.0 mg/L; pH 6.0]

radical scavengers is shown in Fig. 11. The presence of these scavengers, viz., 2-propanol, sodium azide, and sodium biocarbonate, along with the EDTA (shown before) showed a significant decrease in percentage removal of sulfamethoxazole or triclosan from aqueous solutions. This indicated that these radicals are scavenging greatly the involved radical species; therefore, the removal of these pollutants was greatly inhibited. It was therefore affirmed that the •OH radicals were predominantly taking part in the photocatalytic degradation of triclosan. Moreover, the hole was involved to produce the •OH radicals that also degrade the micro-pollutants from aqueous solutions. Similarly, the presence of sodium azide that inhibited the removal of these pollutants showed that the singlet oxygen, possibly, induces the oxidation of triclosan.

Overall the study therefore demonstrates that the absorption of UV-A radiations ($\lambda = 360$ nm) by the nanocomposite Ag NPs/TiO_2 thin film catalyst induces the photocatalytic degradation of sulfamethoxazole or triclosan by the two different mechanistic pathways. UV-A photons cause to excite the electrons from the VB to CB in the TiO_2 semiconductor where the Au(NPs) traps efficiently the excited electrons at the CB. This eventually restricts the recombination of electron/hole pairs in TiO_2 catalyst. The trapped electrons are able to generate the superoxide radical followed by the formation of •OH radicals. On the other hand, the hole that is created in the VB interacts with the O_2 molecule and produces the O_2• radical species. This results the formation of •OH radicals. Therefore, the reactive radical species are predominantly involved in the degradation of micro-pollutants. Similarly, the other possible pathway of degradation is due to the localized surface plasmon resonance effect which produces the electromagnetic field created by the absorption of photon energy by the Au NPs. This electromagnetic field causes the local excitation of the TiO_2 with the generation of electron/hole pairs. Therefore, it again enables the formation of •OH radical, which simultaneously takes part in the degradation of sulfamethoxazole or triclosan from aqueous solutions.

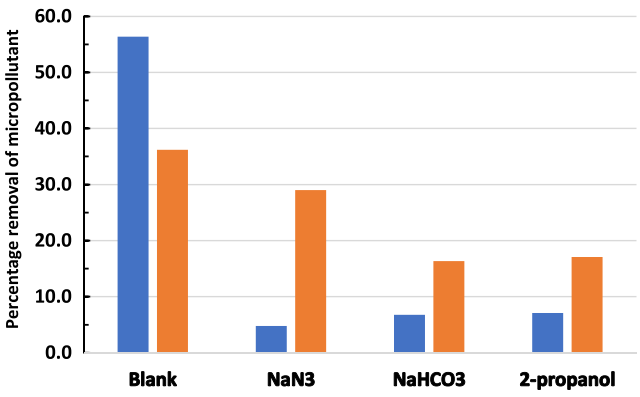

Fig. 11 Photocatalytic degradation of sulfamethoxazole and triclosan in presence of scavengers using the nanocomposite Au NP/TiO_2 thin film photocatalyst ([micro-pollutant] 5.0 mg/L; [scavengers] 1000.0 mg/L; pH 6.0)

Conclusion

Nanocomposite material Au NPs/TiO_2 was synthesized by the template method. SEM image of nanocomposite thin film showed fine grains of TiO_2 were distributed on the surface of borosilicate glass and a heterogeneous structure was obtained. Similarly, the TEM image of nanocomposite powder showed the distribution of gold nanoparticles having the particle size in the range of 25–30 nm and the interplanar distance of the Au nanoparticles 0.25 nm. AFM image of nanocomposite thin film showed that the TiO_2 was making a heterogeneous surface structure on the surface and the root mean square roughness (Rq) and mean roughness (Ra) were found to be 124.33 and 94.66 nm, respectively. The TiO_2 was predominantly possessed the anatase phase with the thin film material. Moreover, the liquid N_2 adsorption/desorption results indicated that the solid was having the H_2 type of hysteresis loop and the pore size, pore volume, and the specific surface area of nanocomposite Au NPs/TiO_2 were found to be 5.60 nm, 0.034 cm^3/g, and 19.91 cm^2/g, respectively. The thin film nanocomposite materials were then successfully utilized in the photocatalytic degradation of emerging micropolltants, viz., sulfamethoxazole and triclosan, from aqueous solutions using the less harmful UV-A light (λ_{max} 360 nm). Increase in solution pH (pH 4.0–8.0) and initial micro-pollutant concentrations (0.5–15.0 mg/L) greatly hampered the percentage removal of these two pollutants both in the photolytic and photocatalytic processes. The kinetic studies showed that the degradation of sulfamethoxazole or triclosan was followed by the pseudo-first-order rate kinetics and increase in concentration from 0.5 to 15.0 mg/L caused to decrease the pseudo-first-order rate constant values from 9.7×10^{-3} to 2.9×10^{-3} min^{-1} (for sulfamethoxazole) and from 8.8×10^{-3} to 1.7×10^{-3} min^{-1} (for triclosan), respectively. Moreover, the degradation of these micro-pollutants followed reasonably well the Langmuir–Hinshelwood isotherm. A significant decrease in percentage of non-purgeable organic carbon (NPOC) was achieved in the photocatalytic degradation of sulfamethoxazole and triclosan. The simultaneous presence of several co-existing ions was tended to affect the removal of these micro-pollutants. Moreover, the presence of 2-propanol, sodium azide, HCO_3^-, and EDTA inhibited significantly the percentage removal of sulfamethoxazole and triclosan from aqueous solutions. This confirmed the active •OH radicals were involved in the degradation process. The stability of nanocomposite thin film was reassessed with the repeated use of catalyst which showed

that no significant decrease in photocatalytic degradation efficiency of these two micro-pollutants from aqueous solutions. Overall, the template-synthesized photocatalyst Au NP/TiO_2 possessed an improved and enhanced catalytic activity in the degradation of emerging micro-pollutants. Moreover, the photocatalytic efficiency was found to be remarkably higher than the photolytic degradation efficiency at least for the removal of sulfamethoxazole and triclosan.

References

Adolfsson-Erici M, Pettersson M, Parkkonen J, Sturve J (2002) Triclosan, a commonly used bactericide found in human milk and in the aquatic environment in Sweden. Chemosphere 46:1485–1489. https://doi.org/10.1016/S0045-6535(01)00255-7

Ahmed MB, Zhou JL, Ngo HH, Guo W (2015) Adsorptive removal of antibiotics from water and wastewater: progress and challenges. Sci Total Environ 532:112–126. https://doi.org/10.1016/j.scitotenv.2015.05.130

Allmyr M, Adolfsson-Erici M, McLachlan MS, Sandborgh-Englund G (2006) Triclosan in plasma and milk from Swedish nursing mothers and their exposure via personal care products. Sci Total Environ 372:87–93. https://doi.org/10.1016/j.scitotenv.2006.08.007

Aranami K, Readman JW (2007) Photolytic degradation of triclosan in freshwater and seawater. Chemosphere 66:1052–1056. https://doi.org/10.1016/j.chemosphere.2006.07.010

Arbuckle TE, Weiss L, Fisher M, Hauser R, Dumas P, Bérubé R, Neisa A, LeBlanc A, Lang C, Ayotte P, Walker M, Feeley M, Koniecki D, Tawagi G (2015) Maternal and infant exposure to environmental phenols as measured in multiple biological matrices. Sci Total Environ 508:575–584. https://doi.org/10.1016/j.scitotenv.2014.10.107

Ayodhya D, Venkatesham M, kumari AS et al (2016) Photocatalytic degradation of dye pollutants under solar, visible and UV lights using green synthesised CuS nanoparticles. J Exp Nanosci 11:418–432. https://doi.org/10.1080/17458080.2015.1070312

Barka N, Qourzal S, Assabbane A, Nounah A, Ait-Ichou Y (2010) Photocatalytic degradation of an azo reactive dye, Reactive Yellow 84, in water using an industrial titanium dioxide coated media. Arab J Chem 3:279–283. https://doi.org/10.1016/j.arabjc.2010.06.016

Behera SK, Kim HW, Oh J-E, Park H-S (2011) Occurrence and removal of antibiotics, hormones and several other pharmaceuticals in wastewater treatment plants of the largest industrial city of Korea. Sci Total Environ 409:4351–4360. https://doi.org/10.1016/j.scitotenv.2011.07.015

Buxton GV, Greenstock CL, Helman WP, Ross AB (1988) Critical review of rate constants for reactions of hydrated electrons, hydrogen atoms and hydroxyl radicals (·OH/·O−) in aqueous solution. J Phys Chem Ref Data 17:513–886. https://doi.org/10.1063/1.555805

Cheng DL, Ngo HH, Guo WS, Liu YW, Zhou JL, Chang SW, Nguyen DD, Bui XT, Zhang XB (2017) Bioprocessing for elimination antibiotics and hormones from swine wastewater. Sci Total Environ 621:1664–1682. https://doi.org/10.1016/j.scitotenv.2017.10.059

Constantin LA, Nitoi I, Cristea NI, Constantin MA (2018) Possible degradation pathways of triclosan from aqueous systems via TiO2 assisted photocatalyis. J Ind Eng Chem 58:155–162. https://doi.org/10.1016/j.jiec.2017.09.020

da Silva BF, Jelic A, López-Serna R et al (2011) Occurrence and distribution of pharmaceuticals in surface water, suspended solids and sediments of the Ebro river basin, Spain. Chemosphere 85:1331–1339. https://doi.org/10.1016/j.chemosphere.2011.07.051

Dias IN, Souza BS, Pereira JHOS, Moreira FC, Dezotti M, Boaventura RAR, Vilar VJP (2014) Enhancement of the photo-Fenton reaction at near neutral pH through the use of ferrioxalate complexes: a case study on trimethoprim and sulfamethoxazole antibiotics removal from aqueous solutions. Chem Eng J 247:302–313. https://doi.org/10.1016/j.cej.2014.03.020

El-Sayed MA (2001) Some interesting properties of metals confined in time and nanometer space of different shapes. Acc Chem Res 34:257–264. https://doi.org/10.1021/ar960016n

Foran CM, Bennett ER, Benson WH (2000) Developmental evaluation of a potential non-steroidal estrogen: triclosan. Mar Environ Res 50:153–156. https://doi.org/10.1016/S0141-1136(00)00080-5

Gee RH, Charles A, Taylor N, Darbre PD (2008) Oestrogenic and androgenic activity of triclosan in breast cancer cells. J Appl Toxicol 28:78–91. https://doi.org/10.1002/jat.1316

Grove C, Liebenberg W, Du JP et al (2003) Improving the aqueous solubility of triclosan by solubilization, complexation, and in situ salt formation. J Cosmet Sci 54:537–550

Guslienko KY (2008) Magnetic vortex state stability, reversal and dynamics in restricted geometries. J Nanosci Nanotechnol 8:2745–2760. https://doi.org/10.1166/jnn.2008.003

Han B, Liu W, Li J, Wang J, Zhao D, Xu R, Lin Z (2017) Catalytic hydrodechlorination of triclosan using a new class of anion-exchange-resin supported palladium catalysts. Water Res 120:199–210. https://doi.org/10.1016/j.watres.2017.04.059

Heath RJ, Rock CO (2000) Microbiology: a triclosan-resistant bacterial enzyme. Nature 406:145–146. https://doi.org/10.1038/35018162

Heath RJ, Li J, Roland GE, Rock CO (2000) Inhibition of the Staphylococcus aureusNADPH-dependent enoyl-acyl carrier protein reductase by triclosan and hexachlorophene. J Biol Chem 275:4654–4659. https://doi.org/10.1074/jbc.275.7.4654

Hu L, Flanders PM, Miller PL, Strathmann TJ (2007) Oxidation of sulfamethoxazole and related antimicrobial agents by TiO2 photocatalysis. Water Res 41:2612–2626. https://doi.org/10.1016/j.watres.2007.02.026

Hu Z, Shao Q, Huang Y, Yu L, Zhang D, Xu X, Lin J, Liu H, Guo Z (2018) Light triggered interfacial damage self-healing of poly(p-phenylene benzobisoxazole) fiber composites. Nanotechnology 29:185602. https://doi.org/10.1088/1361-6528/aab010

Huang X, Tu Y, Song C, Li T, Lin J, Wu Y, Liu J, Wu C (2016) Interactions between the antimicrobial agent triclosan and the bloom-forming cyanobacteria Microcystis aeruginosa. Aquat Toxicol 172:103–110. https://doi.org/10.1016/j.aquatox.2016.01.002

Huang M, Zhang Y, Zhou Y, Zhang C, Zhao S, Fang J, Gao Y, Sheng X (2017) Synthesis and characterization of hollow ZrO2–TiO2/Au spheres as a highly thermal stability nanocatalyst. J Colloid Interface Sci 497:23–32. https://doi.org/10.1016/j.jcis.2017.02.052

Ihara M, Tanaka K, Sakaki K, Honma I, Yamada K (1997) Enhancement of the absorption coefficient of cis-(NCS)2 Bis(2,2′-bipyridyl-4,4′-dicarboxylate)ruthenium(II) dye in dye-sensitized solar cells by a silver island film. J Phys Chem B 101:5153–5157. https://doi.org/10.1021/jp963931z

Jia Y, Wu C, Lee BW, Liu C, Kang S, Lee T, Park YC, Yoo R, Lee W (2017) Magnetically separable sulfur-doped SnFe2O4/graphene nanohybrids for effective photocatalytic purification of wastewater under visible light. J Hazard Mater 338:447–457. https://doi.org/10.1016/j.jhazmat.2017.05.057

Jones RD, Jampani HB, Newman JL, Lee AS (2000) Triclosan: a review of effectiveness and safety in health care settings. Am J Infect Control 28:184–196. https://doi.org/10.1067/mic.2000.102378

Kang AJ, Brown AK, Wong CS, Yuan Q (2018) Removal of antibiotic sulfamethoxazole by anoxic/anaerobic/oxic granular and suspended activated sludge processes. Bioresour Technol 251:151–157. https://doi.org/10.1016/j.biortech.2017.12.021

Karaolia P, Michael-Kordatou I, Hapeshi E, Drosou C, Bertakis Y, Christofilos D, Armatas GS, Sygellou L, Schwartz T, Xekoukoulotakis NP, Fatta-Kassinos D (2018) Removal of antibiotics, antibiotic-resistant bacteria and their associated genes by graphene-based TiO2 composite photocatalysts under solar radiation in urban wastewaters. Appl Catal B Environ 224:810–824. https://doi.org/10.1016/j.apcatb.2017.11.020

Kobayashi M, Kurosu S, Yamaguchi R, Kawase Y (2017) Removal of antibiotic sulfamethoxazole by zero-valent iron under oxic and anoxic conditions: removal mechanisms in acidic, neutral and alkaline solutions. J Environ Manag 200:88–96. https://doi.org/10.1016/j.jenvman.2017.05.065

Kolpin DW, Furlong ET, Meyer MT, Thurman EM, Zaugg SD, Barber LB, Buxton HT (2002a) Pharmaceuticals, hormones, and other organic wastewater contaminants in U.S. streams, 1999−2000: a national reconnaissance. Environ Sci Technol 36:1202–1211. https://doi.org/10.1021/es011055j

Kolpin DW, Furlong ET, Meyer MT, Thurman EM, Zaugg SD, Barber LB, Buxton HT (2002b) Response to comment on "Pharmaceuticals, hormones, and other organic wastewater contaminants in U.S. streams, 1999−2000: a national reconnaissance". Environ Sci Technol 36:4007–4008. https://doi.org/10.1021/es020136s

Kosera VS, Cruz TM, Chaves ES, Tiburtius ERL (2017) Triclosan degradation by heterogeneous photocatalysis using ZnO immobilized in biopolymer as catalyst. J Photochem Photobiol Chem 344:184–191. https://doi.org/10.1016/j.jphotochem.2017.05.014

Lalhriatpuia C, Tiwari D, Tiwari A, Lee SM (2015) Immobilized nanopillars-TiO2 in the efficient removal of micro-pollutants from aqueous solutions: physico-chemical studies. Chem Eng J 281:782–792. https://doi.org/10.1016/j.cej.2015.07.032

Leavey-Roback SL, Krasner SW, Suffet I(M)H (2016) Veterinary antibiotics used in animal agriculture as NDMA precursors. Chemosphere 164:330–338. https://doi.org/10.1016/j.chemosphere.2016.08.070

Li H, Zhang W, Zhang Z, Zhang X (2017) Sorption of triclosan to carbon nanotubes: the combined effects of sonication, functionalization and solution chemistry. Sci Total Environ 580:1318–1326. https://doi.org/10.1016/j.scitotenv.2016.12.095

Li Y, Zhou B, Zheng G, Liu X, Li T, Yan C, Cheng C, Dai K, Liu C, Shen C, Guo Z (2018) Continuously prepared highly conductive and stretchable SWNT/MWNT synergistically composited electrospun thermoplastic polyurethane yarns for wearable sensing. J Mater Chem C 6:2258–2269. https://doi.org/10.1039/C7TC04959E

Lin J, Chen X, Chen C, Hu JT, Zhou CL, Cai XF, Wang W, Zheng C, Zhang PP, Cheng J, Guo ZH, Liu H (2018) Durably antibacterial and bacterially antiadhesive cotton fabrics coated by cationic fluorinated polymers. ACS Appl Mater Interfaces 10:6124–6136. https://doi.org/10.1021/acsami.7b16235

Lindström A, Buerge IJ, Poiger T, Bergqvist PA, Müller MD, Buser HR (2002) Occurrence and environmental behavior of the bactericide triclosan and its methyl derivative in surface waters and in wastewater. Environ Sci Technol 36:2322–2329. https://doi.org/10.1021/es0114254

Liu H, Cao X, Liu G, Wang Y, Zhang N, Li T, Tough R (2013) Photoelectrocatalytic degradation of triclosan on TiO2 nanotube arrays and toxicity change. Chemosphere 93:160–165. https://doi.org/10.1016/j.chemosphere.2013.05.018

Liu H, Li Y, Dai K, Zheng G, Liu C, Shen C, Yan X, Guo J, Guo Z (2015) Electrically conductive thermoplastic elastomer nanocomposites at ultralow graphene loading levels for strain sensor applications. J Mater Chem C 4:157–166. https://doi.org/10.1039/C5TC02751A

Liu H, Dong M, Huang W, Gao J, Dai K, Guo J, Zheng G, Liu C, Shen C, Guo Z (2016) Lightweight conductive graphene/thermoplastic polyurethane foams with ultrahigh compressibility for piezoresistive sensing. J Mater Chem C 5:73–83. https://doi.org/10.1039/C6TC03713E

Liu Z, Liu X, Zheng G, Dai K, Liu C, Shen C, Yin R, Guo Z (2017) Mechanical enhancement of melt-stretched β-nucleated isotactic polypropylene: the role of lamellar branching of β-crystal. Polym Test 58:227–235. https://doi.org/10.1016/j.polymertesting.2017.01.002

Lou X, Lin C, Luo Q, Zhao J, Wang B, Li J, Shao Q, Guo X, Wang N, Guo Z (2017) Crystal structure modification enhanced FeNb11O29 anodes for lithium-ion batteries. ChemElectroChem 4:3171–3180. https://doi.org/10.1002/celc.201700816

Lucida H, Parkin JE, Sunderland VB (2000) Kinetic study of the reaction of sulfamethoxazole and glucose under acidic conditions: I. Effect of pH and temperature. Int J Pharm 202:47–62. https://doi.org/10.1016/S0378-5173(00)00413-0

Ma Y, Lv L, Guo Y, Fu Y, Shao Q, Wu T, Guo S, Sun K, Guo X, Wujcik EK, Guo Z (2017) Porous lignin based poly (acrylic acid)/organo-montmorillonite nanocomposites: swelling behaviors and rapid removal of Pb (II) ions. Polymer 128:12–23. https://doi.org/10.1016/j.polymer.2017.09.009

Martínez S, Morales-Mejía JC, Hernández PP, Santiago L, Almanza R (2014) Solar photocatalytic oxidation of triclosan with TiO2 immobilized on volcanic porous stones on a CPC pilot scale reactor. Energy Procedia 57:3014–3020. https://doi.org/10.1016/j.egypro.2014.10.337

Massé DI, Saady NMC, Gilbert Y (2014) Potential of biological processes to eliminate antibiotics in livestock manure: an overview. Animals 4:146–163. https://doi.org/10.3390/ani4020146

McFarland AD, Haynes CL, Mirkin CA et al (2004) Color my nanoworld. J Chem Educ 81:544A. https://doi.org/10.1021/ed081p544A

Mendioroz S, Pajares JA, Benito I, Pesquera C, Gonzalez F, Blanco C (1987) Texture evolution of montmorillonite under progressive acid treatment: change from H3 to H2 type of hysteresis. Langmuir 3:676–681. https://doi.org/10.1021/la00077a017

Mompelat S, Le Bot B, Thomas O (2009) Occurrence and fate of pharmaceutical products and by-products, from resource to drinking water. Environ Int 35:803–814. https://doi.org/10.1016/j.envint.2008.10.008

Munoz M, de Pedro ZM, Casas JA, Rodriguez JJ (2012) Triclosan breakdown by Fenton-like oxidation. Chem Eng J 198–199:275–281. https://doi.org/10.1016/j.cej.2012.05.097

Muzvidziwa T, Moyo M, Okonkwo O et al (2017) Electrodeposition of zinc oxide nanoparticles on multiwalled carbon nanotube-modified electrode for determination of caffeine in wastewater effluent. Int J Environ Anal Chem 97:1–14. https://doi.org/10.1080/03067319.2017.1337898

Nasseri S, Mahvi AH, Seyedsalehi M, Yaghmaeian K, Nabizadeh R, Alimohammadi M, Safari GH (2017) Degradation kinetics of tetracycline in aqueous solutions using peroxydisulfate activated by ultrasound irradiation: effect of radical scavenger and water matrix. J Mol Liq 241:704–714. https://doi.org/10.1016/j.molliq.2017.05.137

Nguyen LQ, Salim C, Hinode H (2008) Performance of nano-sized Au/TiO2 for selective catalytic reduction of NOx by propene. Appl Catal A Gen 347:94–99. https://doi.org/10.1016/j.apcata.2008.06.002

Noothongkaew S, Han JK, Lee YB, Thumthan O, An KS (2017) Au NPs decorated TiO2 nanotubes array candidate for UV photodetectors. Prog Nat Sci Mater Int 27:641–646. https://doi.org/10.1016/j.pnsc.2017.10.001

Pemberton RM, Hart JP (1999) Electrochemical behaviour of triclosan at a screen-printed carbon electrode and its voltammetric determination in toothpaste and mouthrinse products. Anal Chim Acta 390:107–115. https://doi.org/10.1016/S0003-2670(99)00194-4

Qinzhi H, Jing R, Haijun C et al (2018) Front cover: synergistic hematite-fullerene electron-extracting layers for improved efficiency and stability in perovskite solar cells (ChemElectroChem 5/2018). ChemElectroChem 5:722–722. https://doi.org/10.1002/celc.201800215

Rosu M-C, Coros M, Pogacean F, Magerusan L, Socaci C, Turza A, Pruneanu S (2017) Azo dyes degradation using TiO2-Pt/graphene oxide and TiO2-Pt/reduced graphene oxide photocatalysts under UV and natural sunlight irradiation. Solid State Sci 70:13–20. https://doi.org/10.1016/j.solidstatesciences.2017.05.013

Sanchez-Prado L, Llompart M, Lores M, García-Jares C, Bayona JM, Cela R (2006) Monitoring the photochemical degradation of triclosan in wastewater by UV light and sunlight using solid-phase microextraction. Chemosphere 65:1338–1347. https://doi.org/10.1016/j.chemosphere.2006.04.025

Seaton NA (1991) Determination of the connectivity of porous solids from nitrogen sorption measurements. Chem Eng Sci 46:1895–1909. https://doi.org/10.1016/0009-2509(91)80151-N

Seery MK, George R, Floris P, Pillai SC (2007) Silver doped titanium dioxide nanomaterials for enhanced visible light photocatalysis. J Photochem Photobiol Chem 189:258–263. https://doi.org/10.1016/j.jphotochem.2007.02.010

Shankar A, Salcedo E, Berndt A, Choi D, Ryu JE (2018) Pulsed light sintering of silver nanoparticles for large deformation of printed stretchable electronics. Adv Compos Hybrid Mater 1:193–198. https://doi.org/10.1007/s42114-017-0012-3

Shorke BS, Korake PV, Hankare PP, et al (2018) Synthesis and characterization of pure anatase TiO2 nanoparticles | SpringerLink. https://link.springer.com/article/10.1007%2Fs10854-010-0218-4. Accessed 22 Apr 2018

Singer H, Müller S, Tixier C, Pillonel L (2002) Triclosan: occurrence and fate of a widely used biocide in the aquatic environment: field measurements in wastewater treatment plants, surface waters, and lake sediments. Environ Sci Technol 36:4998–5004. https://doi.org/10.1021/es025750i

Sirés I, Oturan N, Oturan MA, Rodríguez RM, Garrido JA, Brillas E (2007) Electro-Fenton degradation of antimicrobials triclosan and triclocarban. Electrochim Acta 52:5493–5503. https://doi.org/10.1016/j.electacta.2007.03.011

Sivaraman S, Zwahlen J, Bell AF, Hedstrom L, Tonge PJ (2003) Structure−activity studies of the inhibition of FabI, the enoyl reductase from Escherichia coli, by Triclosan: kinetic analysis of mutant FabIs. Biochemistry (Mosc) 42:4406–4413. https://doi.org/10.1021/bi0300229

Son H-S, Ko G, Zoh K-D (2009) Kinetics and mechanism of photolysis and TiO2 photocatalysis of triclosan. J Hazard Mater 166:954–960. https://doi.org/10.1016/j.jhazmat.2008.11.107

Song Z, Wang N, Zhu L, Huang A, Zhao X, Tang H (2012) Efficient oxidative degradation of triclosan by using an enhanced Fenton-like process. Chem Eng J 198–199:379–387. https://doi.org/10.1016/j.cej.2012.05.067

Su T, Shao Q, Qin Z, Guo Z, Wu Z (2018) Role of interfaces in two-dimensional photocatalyst for water splitting. ACS Catal 8:2253–2276. https://doi.org/10.1021/acscatal.7b03437

Sun K, Xie P, Wang Z, Su T, Shao Q, Ryu JE, Zhang X, Guo J, Shankar A, Li J, Fan R, Cao D, Guo Z (2017a) Flexible polydimethylsiloxane/multi-walled carbon nanotubes membranous metacomposites with negative permittivity. Polymer 125:50–57. https://doi.org/10.1016/j.polymer.2017.07.083

Sun Z, Zhang L, Dang F, Liu Y, Fei Z, Shao Q, Lin H, Guo J, Xiang L, Yerra N, Guo Z (2017b) Experimental and simulation-based understanding of morphology controlled barium titanate nanoparticles under co-adsorption of surfactants. CrystEngComm 19:3288–3298. https://doi.org/10.1039/C7CE00279C

Sun K, Fan R, Zhang X, Zhang Z, Shi Z, Wang N, Xie P, Wang Z, Fan G, Liu H, Liu C, Li T, Yan C, Guo Z (2018) An overview of metamaterials and their achievements in wireless power transfer. J Mater Chem C 6:2925–2943. https://doi.org/10.1039/C7TC03384B

Thomaidi VS, Matsoukas C, Stasinakis AS (2017) Risk assessment of triclosan released from sewage treatment plants in European rivers using a combination of risk quotient methodology and Monte Carlo simulation. Sci Total Environ 603–604:487–494. https://doi.org/10.1016/j.scitotenv.2017.06.113

Tian Y, Gao B, Morales VL, Chen H, Wang Y, Li H (2013) Removal of sulfamethoxazole and sulfapyridine by carbon nanotubes in fixed-bed columns. Chemosphere 90:2597–2605. https://doi.org/10.1016/j.chemosphere.2012.11.010

Tiwari D, Lalhriatpuia C, Lalhmunsiama, Lalhriatpuia C, Lalhmunsiama, Lee SM, Kong SH (2015) Efficient application of nano-TiO2 thin films in the photocatalytic removal of Alizarin Yellow from aqueous solutions. Appl Surf Sci 353:275–283. https://doi.org/10.1016/j.apsusc.2015.06.131

Wan Z, Hu J, Wang J (2016) Removal of sulfamethazine antibiotics using CeFe-graphene nanocomposite as catalyst by Fenton-like process. J Environ Manag 182:284–291. https://doi.org/10.1016/j.jenvman.2016.07.088

Wang J, Wang S (2016) Removal of pharmaceuticals and personal care products (PPCPs) from wastewater: a review. J Environ Manag 182:620–640. https://doi.org/10.1016/j.jenvman.2016.07.049

Wang C, Zhao M, Li J, Yu J, Sun S, Ge S, Guo X, Xie F, Jiang B, Wujcik EK, Huang Y, Wang N, Guo Z (2017) Silver nanoparticles/graphene oxide decorated carbon fiber synergistic reinforcement in epoxy-based composites. Polymer 131:263–271. https://doi.org/10.1016/j.polymer.2017.10.049

Wang X, Liu X, Yuan H, Liu H, Liu C, Li T, Yan C, Yan X, Shen C, Guo Z (2018a) Non-covalently functionalized graphene strengthened poly(vinyl alcohol). Mater Des 139:372–379. https://doi.org/10.1016/j.matdes.2017.11.023

Wang Y, Fang Y, Lu W, Li N, Chen W (2018b) Oxidative removal of sulfa antibiotics by introduction of activated carbon fiber to enhance the catalytic activity of iron phthalocyanine. Microporous Mesoporous Mater 261:98–104. https://doi.org/10.1016/j.micromeso.2017.10.055

Wu Q, Shi H, Adams CD, Timmons T, Ma Y (2012) Oxidative removal of selected endocrine-disruptors and pharmaceuticals in drinking water treatment systems, and identification of degradation products of triclosan. Sci Total Environ 439:18–25. https://doi.org/10.1016/j.scitotenv.2012.08.090

Xu D, Liu K, Shi W et al (2015) Ag-decorated K2Ta2O6 nanocomposite photocatalysts with enhanced visible-light-driven degradation activities of tetracycline (TC). Ceram Int 3(Part B):4444–4451. https://doi.org/10.1016/j.ceramint.2014.11.136

Yang B, Ying G-G, Zhao J-L, Zhang LJ, Fang YX, Nghiem LD (2011) Oxidation of triclosan by ferrate: reaction kinetics, products identification and toxicity evaluation. J Hazard Mater 186:227–235. https://doi.org/10.1016/j.jhazmat.2010.10.106

Yang Y, Lu X, Jiang J, Ma J, Liu G, Cao Y, Liu W, Li J, Pang S, Kong X, Luo C (2017) Degradation of sulfamethoxazole by UV, UV/H2O2 and UV/persulfate (PDS): formation of oxidation products and effect of bicarbonate. Water Res 118:196–207. https://doi.org/10.1016/j.watres.2017.03.054

Yoon J-W, Baek M-H, Hong J-S, Lee CY, Suh JK (2012) Photocatalytic degradation of azo dye using TiO_2 supported on spherical activated carbon. Korean J Chem Eng 29:1722–1729. https://doi.org/10.1007/s11814-012-0076-2

Yu JC, Kwong TY, Luo Q, Cai Z (2006) Photocatalytic oxidation of triclosan. Chemosphere 65:390–399. https://doi.org/10.1016/j.chemosphere.2006.02.011

Yuval A, Eran F, Janin W, Oliver O, Yael D (2017) Photodegradation of micropollutants using V-UV/UV-C processes; Triclosan as a model compound. Sci Total Environ 601–602:397–404. https://doi.org/10.1016/j.scitotenv.2017.05.172

Zhang L, Qin M, Yu W, Zhang Q, Xie H, Sun Z, Shao Q, Guo X, Hao L, Zheng Y, Guo Z (2017a) Heterostructured TiO2/WO3

nanocomposites for photocatalytic degradation of toluene under visible light. J Electrochem Soc 164:H1086–H1090. https://doi.org/10.1149/2.0881714jes

Zhang L, Yu W, Han C, Guo J, Zhang Q, Xie H, Shao Q, Sun Z, Guo Z (2017b) Large scaled synthesis of heterostructured electrospun TiO2/SnO2 nanofibers with an enhanced photocatalytic activity. J Electrochem Soc 164:H651–H656. https://doi.org/10.1149/2.1531709jes

Zhao J, Wu L, Zhan C, Shao Q, Guo Z, Zhang L (2017) Overview of polymer nanocomposites: computer simulation understanding of physical properties. Polymer 133:272–287. https://doi.org/10.1016/j.polymer.2017.10.035